CMS Physics Analysis Summary

2008/10/06

SUSY searches with dijet events

The CMS Collaboration

Abstract

A search for supersymmetry (SUSY) in dijet events with the CMS detector at the LHC is presented. This study is focused on a SUSY parameter space where squarks are pair produced and both decay directly to a quark and a neutralino. The latter escapes undetected and gives rise to the celebrated missing energy signature of supersymmetry. Although the background from QCD dijet events is overwhelming, the particular kinematics of the SUSY events allow powerful discriminating variables to be defined which should enable an early discovery with the first collision data.

1 Introduction

In this note, search strategies are presented for a possible discovery of supersymmetric (SUSY) signatures at the LHC using dijet events. A new approach to SUSY searches with dijet events was recently proposed in Ref. [1]. It is based on the assumption that squarks are pair produced and subsequently decay directly to a quark and the χ_1^0, the lightest stable particle (LSP). This approach is most promising for regions in SUSY parameter space where squarks have large branching fractions to decay directly to the LSP. This configuration in turn requires the gluino to be heavier than the squarks, thus avoiding cascade decays of squarks via the gluino. Therefore the event topology under investigation consists of two high-p_T jets and two invisible neutralinos which lead to a missing energy signature. The main background processes for this topology are QCD dijet events and Z + jet events where the Z decays into two neutrinos. It is however possible to define kinematic variables that can discriminate between signal and background without relying on the missing energy measurement from the calorimeters. The analysis presented in this note is an extension to the existing SUSY searches within CMS which so far have focused on missing E_T signatures with at least three jets and/or involving charged leptons [2].

2 Data Samples and event selection

The signal and background samples simulated for this analysis have been taken from the CSA07 data challenge [3]. The background data can be divided into three main data sets:

- QCD processes generated using PYTHIA [4], including minimum bias and high-energy jet data.
- $t\bar{t}$ + jets, W + jets, and Z + jets events (excluding $Z \to \nu\bar{\nu}$), all simulated using ALPGEN [5]
- Z + jets events with $Z \to \nu\bar{\nu}$, generated with PYTHIA

In addition, single top, γ + jets and $b\bar{b}$ + jets background samples were investigated which, however, only play a negligible role in the presented search. Possible SUSY signal yields are estimated using the CMS low mass mSuGra points LM1 – LM4, defined in Table 1.

Table 1: Definition of low mass SUSY points. Cross sections were estimated using PROSPINO1 [6]. The last two columns give the masses of the lightest squark and the lightest neutralino, χ_1^0.

Sample	m_0 (GeV)	$m_{1/2}$ (GeV)	A_0	$\tan\beta$	sign(μ)	σ NLO (pb)	(LO) (pb)	lightest $\tilde{q}$ (GeV)	χ_1^0 (GeV)
LM1	60	250	0	10	+	54.86	(43.28)	410 ($\tilde{t}_1$)	97
LM2	185	350	0	35	+	9.41	(7.27)	582 ($\tilde{t}_1$)	141
LM3	330	240	0	20	+	45.47	(34.20)	446 ($\tilde{t}_1$)	94
LM4	210	285	0	10	+	25.11	(19.43)	483 ($\tilde{t}_1$)	112

The trigger requirement and physics object definitions used in this analysis are as follows:

- Trigger:
  Events are required to pass a two-jet trigger, "HLT2jet", where the Level 1 trigger conditions are either "L1_SingleJet150" or "L1_DoubletJet70" (i.e. either one jet with E_T greater than 150 GeV or two jets with E_T greater than 70 GeV). At the High Level

Trigger this cut is raised to two jets with E_T greater than 150 GeV, significantly higher than the preselection cuts in this analysis, but a necessary consequence of the current trigger pathways.

- Jet definitions:
  For calorimeter jet clustering, the corrected iterative cone algorithm with $R = 0.5$ is used where multiple candidates, jet-electron overlaps and jet-muon overlaps have been resolved [7]. Two jets with $p_T > 50\,\text{GeV}$ are required and the electromagnetic fraction F_{em} must be less than 0.9.
- Missing momentum based on jets:
  Based on the two leading jets two additional variables are defined: HT as the scalar sum of the two leading jet p_T's, $\text{HT} = p_T^{j1} + p_T^{j2}$ and missing p_T (MHT) of the event calculated as $\vec{\text{MHT}} = -(\vec{p}_T^{\,j1} + \vec{p}_T^{\,j2})$.
- Lepton veto:
  Any event where either an isolated electron or muon with momentum $p_T > 10\,\text{GeV}$ was identified is vetoed.
- Additional jet veto:
  In order to select "clean" dijet events, events with any additional jets with $p_T > 50\,\text{GeV}$, which also includes jets from hadronic τ decays, are vetoed too.

To protect against significant mis-measurements of jet energies, events where the missing p_T based on the two jet system points into the same direction as one of the first three jets, are rejected, by requiring $\Delta\phi(\text{j}, \text{MHT}) < 0.3$ rad. This definition of missing E_T based on the two jet momenta should also be robust against fake signals and noise in the calorimeters. In addition to the selection criteria above, the leading jet must be within $|\eta| < 2.5$.

To summarize, the following preselection is applied:

- $p_T^{j1} > 50\,\text{GeV}$, $p_T^{j2} > 50\,\text{GeV}$
- $F_{em}^{j1} < 0.9$, $F_{em}^{j2} < 0.9$
- $|\eta_{j1}| < 2.5$
- $p_T^{j3} < 50\,\text{GeV}$
- $\Delta\phi(\text{j}_i, \text{MHT}) < 0.3$ rad (i=1,2,3)
- $p_T^e < 10\,\text{GeV}$, $p_T^\mu < 10\,\text{GeV}$

3 Analysis Method and results

3.1 Event kinematics

As mentioned in the previous section the "HLT2jet" trigger requires already two (uncorrected) jets with $p_T > 150\,\text{GeV}$ each, which implies $\text{HT} \gtrsim 300\,\text{GeV}$. For signal events two high-p_T jets come directly from a squark decay with typical mass of the order of 600 GeV. Therefore, to make the analysis cuts more restrictive than the trigger and to further reduce background contributions it is required that HT exceeds 500 GeV.

Even after requiring two high-p_T jets, sizeable background contributions from a number of processes remain, the most important of which are:

- QCD dijet events due to their (overwhelmingly) large cross section and sizeable uncertainties in higher-oder corrections, in particular production of extra jets due to

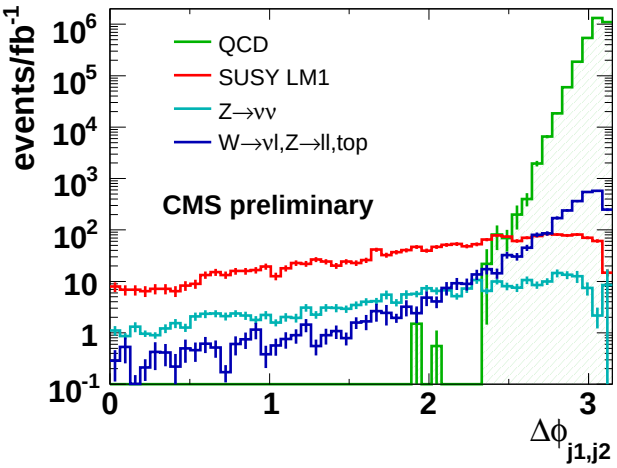

Figure 1: Distribution of $\Delta\phi_{j1,j2}$, after application of all selection cuts apart from the one on α (α_T).

gluon emission;

- $Z \to \nu\bar{\nu}$ events which present an irreducible background as the invisible Z decay leads to real missing E_T;
- W + jets events, where the W decays leptonically and the charged lepton was either not reconstructed or outside the detector acceptance.

It is however possible to define kinematic variables to disentangle QCD events and signal-like events with real missing E_T. In well measured QCD dijet events, transverse momentum conservation requires the p_T of the two jets to be of equal magnitude and back-to-back in the plane transverse to the beam. In contrast, in signal-like events the two squarks decay independently of each other and therefore the resulting jet p_T's can be of different magnitude and their ϕ values (largely) uncorrelated. The difference in the azimuthal angle ϕ for the background processes and the low mass SUSY point LM1 is shown in Fig. 1.

In Ref. [1], a new variable α was suggested which exploits the requirement of back-to-back jets of equal magnitude for QCD events:

$$\alpha = E_T^{j2} / M_{inv}^{j1,j2} . \tag{1}$$

For massless particles this is equal to

$$\alpha = \frac{E_T^{j2}}{\sqrt{2E^{j1}E^{j2}(1-\cos\Theta)}} , \tag{2}$$

where Θ is the angle between the two jets. As can be seen from Eq. 2, α can at most have a value of 0.5 for well measured QCD events. In addition, as the E_T of the second energetic jet enters in the numerator, uncertainties introduced through energy mis-measurements partly cancel out in α. (If one of the two jet energies is mis-measured by a large amount, the order of the two jets is reversed.) A modified version of this variable is also explored in which the transverse mass of the two jets is used instead of the invariant mass:

$$\alpha_T = E_T^{j2} / M_{inv\ T}^{j1,j2} , \tag{3}$$

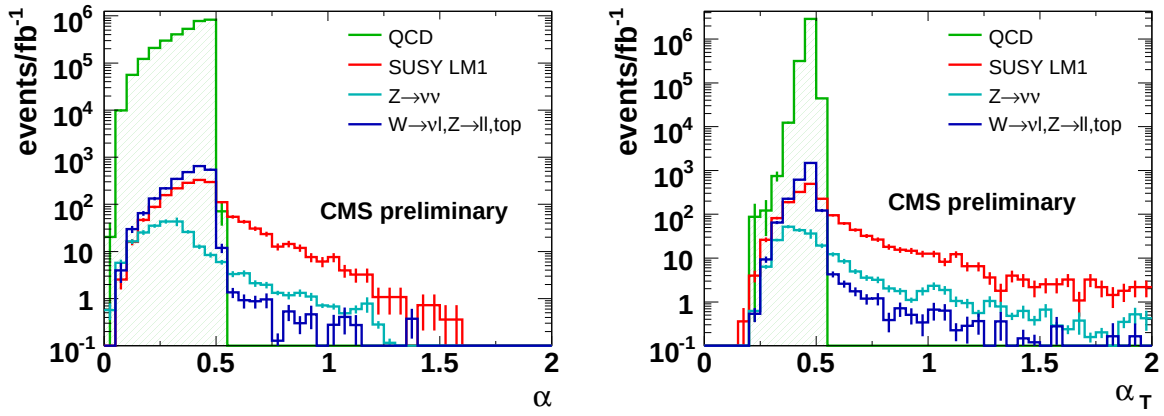

Figure 2: Distribution of α and α_T after all other selection cuts have been applied.

Again, for massless particles, this equation can be rewritten as

$$\alpha_T = \frac{E_T^{j2}}{\sqrt{2E_T^{j1}E_T^{j2}(1-\cos\Delta\phi)}} = \frac{\sqrt{E_T^{j2}/E_T^{j1}}}{\sqrt{2(1-\cos\Delta\phi)}} \tag{4}$$

where $\Delta\phi$ is the difference in azimuthal between the two jets. For well measured QCD dijet events, α_T is exactly 0.5. The α and α_T distributions are shown in Fig. 2 for the different background processes and exemplary for LM1.

While the inspection of Fig. 1 might lead to simply require $\Delta\phi \lesssim 2\pi/3$ rad, it was preferred here to use α and α_T instead. In the particular case of QCD dijet events, additional hard and soft gluon emission is associated with significant uncertainties, which alters the $\Delta\phi$ distribution for such events. A detailed study by the DØ experiment [8] found sizeable differences in the modeling of these higher-order effects by Monte-Carlo event generators when compared with the data. While the present selection is safe with respect to the effects of hard extra gluon radiation by rejecting events with extra jets with $p_T > 50\,\text{GeV}$, multiple soft gluon emission might still noticeably effect the $\Delta\phi$ distribution. Compared with $\Delta\phi$, α and α_T have the additional benefit that they are more effective in rejecting $Z \to \nu\bar{\nu}$ events. In the following α and α_T, shown in Fig. 2 are used in the event selection. These variables also reject events where the p_T of the two jets is not balanced. Both variables are highly correlated to $\Delta\phi$, i.e. an additional cut on $\Delta\phi$ has a negligible effect.

To account for finite jet energy and ϕ resolution it is required that $\alpha\,(\alpha_T)$ exceeds 0.55. To summarize the following cuts are applied on top of the preselection:

- $HT > 500\,\text{GeV}$
- $\alpha > 0.55$ or $\alpha_T > 0.55$ and $\Delta\phi_{j1,j2} < 2\pi/3$ rad.

3.2 Expected event yields from Simulations

After the selection criteria described above are applied, the event yields listed in Table 2 are obtained for background events and the LM1 signal point. All the numbers correspond to an integrated luminosity of $1\,\text{fb}^{-1}$.

Both α and α_T are very effective in reducing the backgrounds, particularly from QCD dijet events but also for electroweak processes. When α_T is used instead of α, the signal yield for

Table 2: Numbers of expected events after each selection cut for background samples (QCD, $t\bar{t}$, W, Z + jets, and $Z \to \nu\bar{\nu}$) and LM1 signal point. The final numbers of events selected are shown after a cut on α or alternatively α_T and $\Delta\phi_{j1,j2}$.

Selection cut	QCD	$t\bar{t}$,W,Z	$Z \to \nu\bar{\nu}$	LM1
Trigger	1.1×10^8	147892	1807	25772
Preselection	3.4×10^7	9820	878	2408
HT > 500 GeV	3.2×10^6	2404	243	1784
$\alpha > 0.55$	0	7.2	19.7	227.6
$\alpha_T > 0.55$	0	19.9	58.2	439.6
$\Delta\phi_{j1,j2} < 2\pi/3$	0	18.7	57.2	432.4

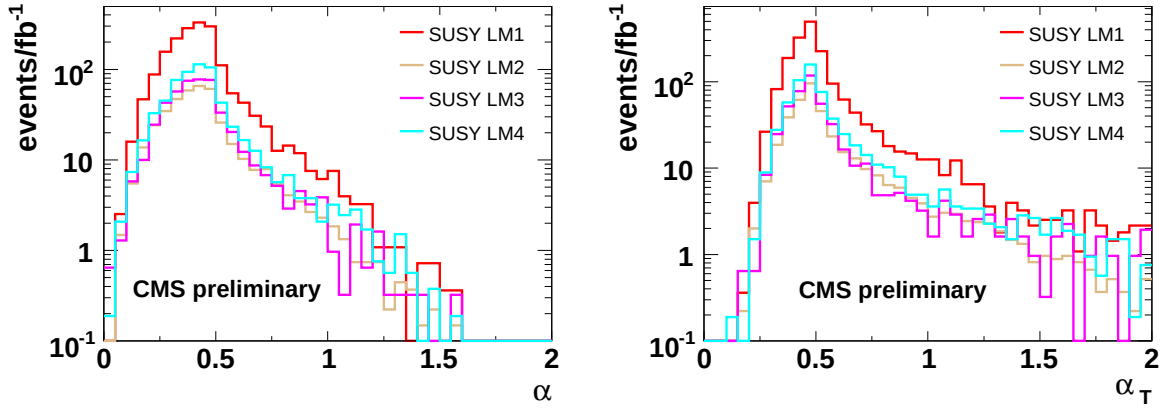

Figure 3: Distribution of α and α_T for the different low mass SUSY points after all other selection cuts have been applied.

the LM1 point is almost doubled. The dominant background from $Z \to \nu\bar{\nu}$ however rises by about a factor 3 while the background from $t\bar{t}$, W, and Z decays doubles as well. It is therefore proposed to study both variables with real data as the signal to background ratio differs in the two cases. Nevertheless, in each case signal over background ratios larger than 5.0 are expected.

Beside the mSuGra point LM1, the event yields for the low mass SUSY points LM2 – LM4 were studied and are summarised in Table 3. Here, only the selection on α_T was used. Figure 3 shows the α and α_T distributions for the LM points studied.

From Table 3, it can be seen that also for LM4 a signal-over-background ratio in excess of 2 can be achieved while for LM2 and LM3, the signal would still dominate over the expected background. In addition to the expected event yields, the underlying production process and subsequent decay for events surviving the selection criteria were studied to verify that the selection is mainly sensitive to the decay $\tilde{q} \to \chi_1^0 q$. The following 5 categories are defined:

- $\tilde{q}\,\tilde{q}$ (invisible):
  production process is $\tilde{q}\,\tilde{q}$ and both squarks decay to quark + invisible, either directly via $\tilde{q} \to \chi_1^0 q$ or $\tilde{q} \to \chi_2^0 q$ followed by $\chi_2^0 \to \chi_1^0 \nu\bar{\nu}$
- $\tilde{q}\,\tilde{q}$ (other):
  production process is $\tilde{q}\,\tilde{q}$ where at least one of the squarks decays to a quark + visible particles

- $\tilde{q}\,\tilde{g}$: production process is $\tilde{q}\,\tilde{g}$
- $\tilde{g}\,\tilde{g}$: production process is $\tilde{g}\,\tilde{g}$
- other : all other production processes

The results are summarized in Table 3. It can be seen that for most of the models studied, the pair production of squarks and their subsequent decay to a quark + invisible particles is the dominant contribution. The relatively large contributions from $\tilde{q}\,\tilde{q}$ (other) can be attributed to χ_1^+ decays to χ_1^0 in which, due to the small mass differences, a low p_T charged lepton is produced that remains undetected.

Table 3: Event yields expected for specific low mass SUSY points after selection on $\not{\alpha}_T$ normalised to 1 fb^{-1}. The relative contribution from the different production processes to the selected signal is also shown.

Sample	Events	$\tilde{q}\,\tilde{q}$ (invisible)	$\tilde{q}\,\tilde{q}$ (other)	$\tilde{q}\,\tilde{g}$	$\tilde{g}\,\tilde{g}$	other
LM1	432	39%	22%	34%	3%	1%
LM2	132	46%	33%	18%	0%	2%
LM3	138	69%	17%	12%	0%	2%
LM4	195	49%	10%	36%	3%	1%

Table 4: Relative contribution of different production processes for the LM1 point when varying the requirement on the third jet p_T.

Production process	$p_T^{j3} < 30$ GeV	$p_T^{j3} < 50$ GeV	$p_T^{j3} < 70$ GeV
$\tilde{q}\,\tilde{q}$	80%	61%	51%
$\tilde{q}\,\tilde{g}$	18%	34%	44%
$\tilde{g}\,\tilde{g}$	1%	3%	5%

The contribution from $\tilde{q}\,\tilde{g}$ production can be attributed to $\tilde{g} \to \tilde{q}q$ decays where the additional jet from the $\tilde{g}$ decay is relatively soft because of the small mass difference between $\tilde{q}$ and $\tilde{g}$. To test this assumption the requirement on the p_T of the third jet was varied by ± 20 GeV. The results are shown in Table 4 for LM1. The contribution from $\tilde{q}\,\tilde{q}$ is enhanced when lowering the third jet veto to 30 GeV while it is reduced when increased to 70 GeV.

3.3 Jet-energy scale and resolution uncertainties

The systematic uncertainties due to miscalibration and mismeasurement of jets were estimated by applying the following systematic variations:

- A Gaussian smearing of the transverse jet momenta of 10% and a Gaussian smearing of the azimuthal angle ϕ by 0.1 rad;
- A scaling of the jet energy scale by $\pm$ 5%;
- A scaling of the jet energy scale in the forward direction ($|\eta| > 1.4$) by $\pm$ 3%.

It was found that the Gaussian smearing only has a small effect ($\sim$ 3%) on the selected signal and background events. The upward scaling of the transverse momenta of the jets effectively relaxes the HT cut and hence more events pass the selection. Conversely, the reduced momentum therefore leads to fewer events. The largest deviation is a 12% reduction in both, the signal and background efficiencies, leaving the signal-over-background ratio largely unchanged. The

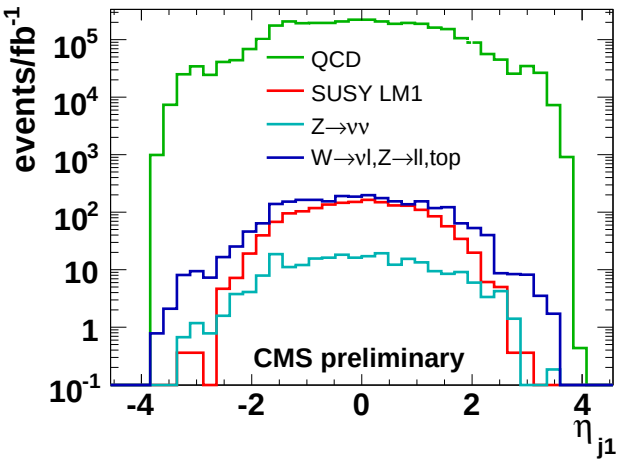

Figure 4: Distribution of η for QCD, $t\bar{t}$, W, Z, and SUSY events. Shown is the expected number of events for a luminosity of 1fb^{-1}, after all selection cuts except the cut on α_T and $|\eta_{j1}|$.

miscalibration applied for the jet energy scale in the forward regions has a negligible effect. Overall the signal-to-background ratio remains stable under varying conditions and the background from QCD remains small in all scenarios.

4 Data-driven background estimation

In the following, the data-driven methods for background estimate in this analysis are described. The main emphasis is on an approach where signal enhanced and depleted regions in phase space are defined and the combination of all backgrounds can be estimated simultaneously. In a second approach, which can serve as a cross check, it is described how $W \to \mu\nu$ events can be used to determine the size of the dominant $Z \to \nu\bar{\nu}$ background. The background estimations described here are carried out for an event selection using α_T

4.1 Background estimation using the η dependence of α_T via the matrix method

The idea of the matrix method is to find two variables, $\mathcal{V}_1$ and $\mathcal{V}_2$, which are uncorrelated for background events and for which in the 2-d plane three quadrants exists that are signal depleted and one that is signal enriched, i.e., each variable has a signal-enriched and a signal-depleted region. In this case it is possible to determine the amount of background events directly from the data.

The two variables in question for the present analysis are the pseudo-rapidity $|\eta|$ of the leading jet and α_T. As can be seen from Fig. 4, the leading jet from a SUSY event is on average more central than those from the background processes, QCD, $t\bar{t}$, W, Z + jets and $Z \to \nu\bar{\nu}$.

Therefore, the forward regions with $|\eta| > 2.5$ are considered as signal depleted. Similarly, the region formed by $\alpha_T > 0.55$ is signal enriched while that with $\alpha_T < 0.55$ is signal depleted. The variable $R^i_{\alpha_T} = N_{\alpha_T>0.55}/N_{\alpha_T<0.55}$ is defined as the ratio of events with $\alpha_T > 0.55$ to those with $\alpha_T < 0.55$ for a given bin i in $|\eta|$. It needs to be constant for the method outlined above to be applicable.

In real data, it will not be possible to distinguish the different background processes on an event-by-event basis. It was observed that R_{α_T} is, to a good approximation, constant for all the

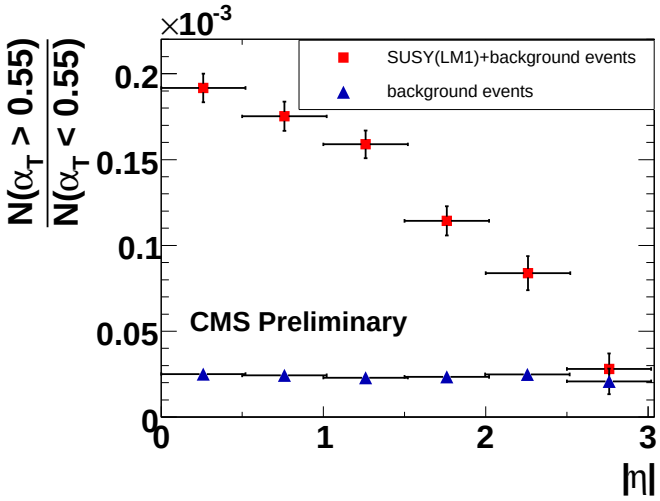

Figure 5: R_{α_T} as a function of $|\eta|$ of the leading jet after all selection cuts except the cut on α_T and $|\eta|$. Shown once for background events only (blue triangles) and for a mixture of background and SUSY events for LM1 (red squares).

Table 5: Numbers of events simulated with $\alpha_T > 0.55$ and $|\eta| < 2.5$ compared to the numbers of background events determined using the matrix method. The errors refer to statistical uncertainties due to the finite size of the samples of events simulated. In parentheses are the expected statistical uncertainties for a data sample of 1fb^{-1}.

Simulated background ($\alpha_T > 0.55$ and $\|\eta\| < 2.5$)	Predicted background no SUSY contribution	Simulated background and SUSY(LM1)	Predicted background SUSY (LM1) contamination
$77 \pm 3\ (\pm 8)$	$68 \pm 24\ (\pm 43)$	$517 \pm 13\ (\pm 22)$	$91 \pm 30\ (\pm 51)$

relevant background contributions. It is therefore legitimate to combine all the backgrounds and determine the sum of all backgrounds with the help of the matrix method.

In Fig. 5, R_{α_T} is shown for all backgrounds combined. As can be seen also the "combined R_{α_T}" is flat as a function of $|\eta|$. The value of R_{α_T} determined in the forward region $|\eta| > 2.5$ is $R_{\alpha_T} = (1.7 \pm 0.1) \cdot 10^{-5}$. In addition, R_{α_T} is shown for the case of a LM1 signal present in the data.

To estimate the number of background events in the $|\eta| < 2.5$ regions, $N_{\text{pred}}(|\eta|)$, R_{α_T} needs to be multiplied with the number of of events with $\alpha_T < 0.55$, $N_{\text{bkgd}}(|\eta|)$, in the corresponding $|\eta|$ bin:

$$N_{\text{pred}}(|\eta|) = R_{\alpha_T} \cdot N_{\text{bkgd}}(|\eta|)\,.$$

Figure 6 shows the numbers of background events predicted and measured after all selection cuts in the different $|\eta|$ regions. The two distributions agree very well within errors. In Fig. 6, the number of signal-plus-background events is also compared to the number of background events predicted. A signal is clearly visible above the background.

In Table 5, the absolute numbers of background events predicted and simulated in the signal region $|\eta| < 2.5$ and $\alpha_T > 0.55$ are given. The prediction is done once in the case that SUSY is realised in nature at parameter-point LM1 and once for the case that SUSY is not realised in nature. If no signal is present, the background can be predicted within the simulated statistical precision. The presence of a SUSY signal leads to a slight overestimate of the background.

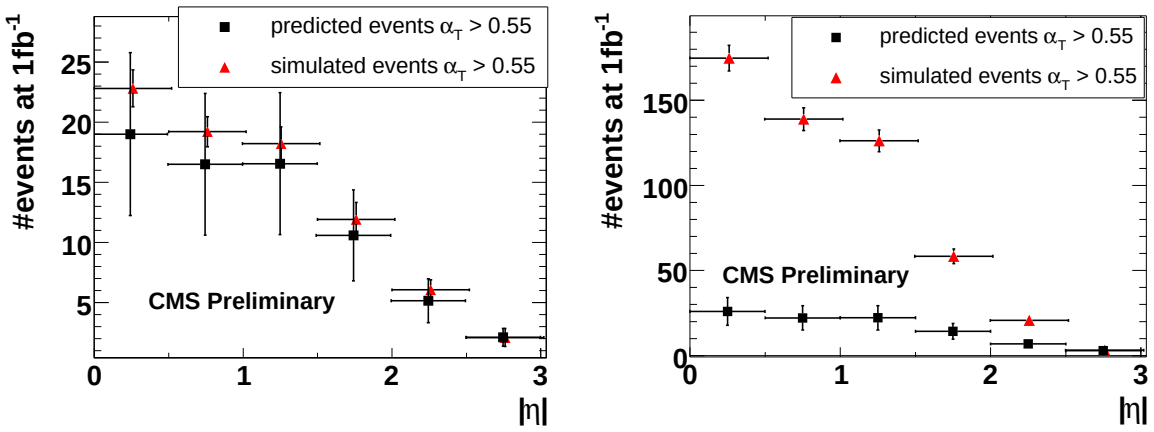

Figure 6: Comparison of the numbers of events predicted and simulated for a luminosity of 1 fb^{-1} with $\alpha_T > 0.55$. Left: Background events only. The black squares indicate the number of events predicted, the number of events simulated is shown as red triangles. Right: number of background events predicted in the presence of signal contamination from LM1 (black squares) and the total number of events observed in the region $\alpha_T > 0.55$ (red triangles) in presence of LM1.

Despite the large statistical uncertainty on the background prediction, a clear signal would however still be visible. The stability of the presented matrix method was verified against the systematic variations discussed in Sec. 3.3.

4.1.1 Validation of the Matrix Method with real data

The validity of this method can be estimated directly from data. To do so, the selection cuts are loosened until the signal contribution becomes negligible compared to the backgrounds. Then R_{α_T} should be independent of $|\eta|$.

Figure 7 shows R_{α_T} for a mix of SUSY LM1 and background events for several different HT cuts. For relatively low requirements on HT, R_{α_T} stays approximately constant while for stricter requirements on HT, R_{α_T} is falling off with larger values of $|\eta|$. Figure 8 shows the same plot for loosened cuts on the third leading jet p_T. Here the ratio changes with the cut on the third jet p_T as more genuine three jets events are selected for which α_T can have values greater than 0.55. Again, for cuts on p_T^{j3} where the signal contribution is negligible R_{α_T} is flat as a function of $|\eta|$ while for more strict vetoes on the third jet a clear slope in R_{α_T} is visible.

These studies present elementary checks that will need to be carried out once real collision data are available.

4.2 Estimating the Z $\rightarrow \nu\bar{\nu}$ background with the help of W + jets events

It is possible to estimate the jets + Z to invisible background from the W + jets channel. Such a study can be used as cross check of the forward extrapolation method discussed in the previous section. Given the larger cross section, W's will be reconstructed with greater statistics than Z's. Once a clean W sample is selected it still needs to be normalised to the Z's, which can be done either from data or with the help of Monte-Carlo simulations. Except for the W identification via an isolated muon, the selection is kept exactly the same as for the final analysis. Similar strategies have been studied in detail for SUSY searches involving three and more jets [9].

The W + jets events are selected by identifying an isolated global muon. For muon isolation

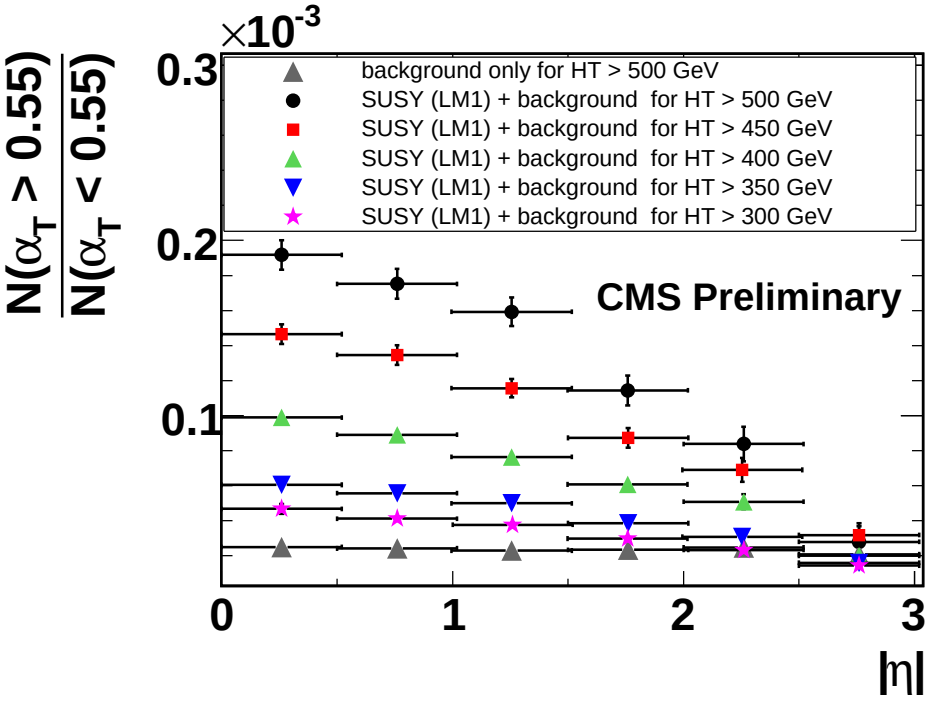

Figure 7: R_{α_T} as a function of $|\eta|$ for different HT cuts.

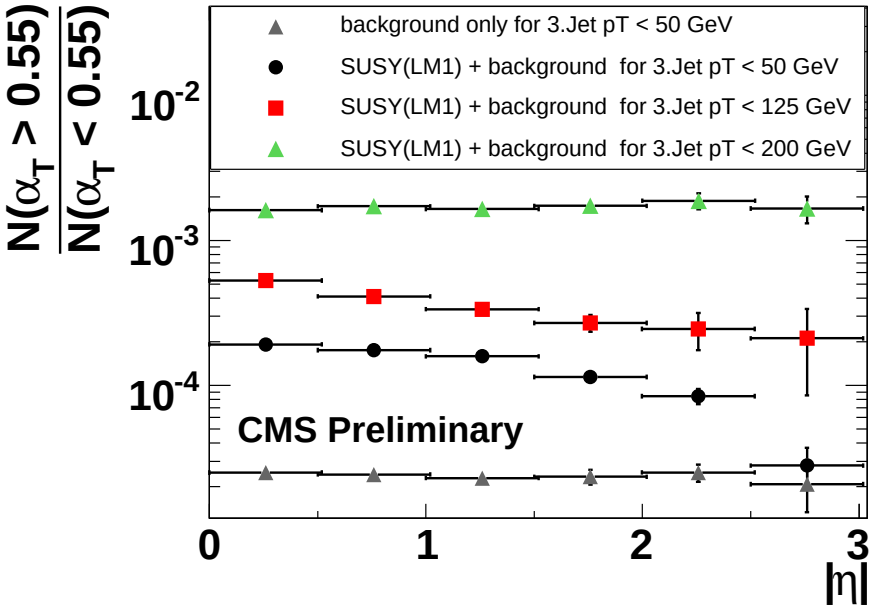

Figure 8: R_{α_T} as a function of $|\eta|$ for different cuts on the p_T of the third leading jet.

the same method as proposed for the W cross section measurement [10] is used and similarly in the Z to invisible background estimate for SUSY searches with larger jet multiplicities [9]. Muons are selected with transverse momentum greater than 25 GeV leaving the remaining event selection cuts unchanged. This selection leads to a clean W sample of 48.7 events with a purity of 92%. The only remaining backgrounds are $t\bar{t}$ (3.2 events) and a small amount of Z + jets (0.9 events). To protect against muons from SUSY decays, the fact that W's satisfying the α_T cut have transverse momenta of a few 100 GeV is exploited. For these events, the p_T and ϕ of the muon is correlated to MHT and hence we require $p_{T\mu}/\text{MHT} > 0.25$ and $\Delta\phi(\mu, \text{MHT}) < 0.75$ rad. These requirements result in a clean sample of W candidates, W_{cand}, of 40 events with 94% purity and no SUSY LM1 contamination. Pairs of global muons with an invariant mass within a 10 GeV window of the nominal Z mass are selected as Z candidates, Z_{cand}. This selection is 100% pure and 3.6 events are expected after application of all selection criteria for $1\,\text{fb}^{-1}$.

The number of true $Z \to \nu\bar{\nu}$ events can be estimated as:

$$Z \to \nu\bar{\nu}_{\text{estimated}} = W_{\text{cand}} \times W_{\text{true}}/W_{\text{cand}} \times Z_{\text{true}}/W_{\text{true}} \times 6 = 61.6 \pm 10.1$$

where the factor 6 in Eq. 4.2 stems from the Standard Model relation for the ratio of $Z \to \nu\bar{\nu}$ to $Z \to \mu\mu$. W_{true} (Z_{true}) is the true number of $W \to \mu\nu$ ($Z \to \mu\mu$) events in the simulated sample that survive the standard selection (without muon veto).

The number of W events observed is acceptance- and efficiency-corrected to obtain the true number of W's in the data sample. With the early collision data of the LHC, it will be possible to take the ratio of true W's and true Z's in the two-jet channel from tuned simulations. The numbers used in our study for the determination of the $Z \to \nu\bar{\nu}$ background are shown in Table 6. The quoted uncertainty is statistical only.

The ratio of W/Z taken from the simulation might, however, have large uncertainties and a determination from the data may be preferable if sufficient statistics are available. To increase the statistics of the reconstructed W's and Z's, the HT cut is relaxed to HT > 300 GeV. This cut leads to 187 W candidates, of which 18 are $t\bar{t}$ and 3 Z + jets events, and 20 Z candidates with 100% purity. The events selected this way are close enough in phase space to assume a constant ratio of Z/W for the two HT requirements. Only 0.7 events of the LM1 SUSY sample passed the relaxed cuts. The limiting factor of this method is the statistical uncertainty due to the small number of reconstructed Z. This method would lead to an estimation of 65.4 ± 16.9 $Z \to \nu\bar{\nu}$ events. Compared to the quoted uncertainty, the uncertainty from acceptance and efficiency is negligible. The expected numbers of $Z \to \nu\bar{\nu}$ background events from this closure test agrees well with the 58.2 $Z \to \nu\bar{\nu}$ events expected in the presented SUSY search.

Table 6: W and Z after final cuts in from Monte Carlo truth and reconstruction.

	W_{cand}	$W_{\text{true}}/W_{\text{cand}}$	Z_{cand}	$Z_{\text{true}}/Z_{\text{cand}}$	$Z_{\text{true}}/W_{\text{true}}$	$Z \to \nu\bar{\nu}$
HT > 300 GeV	186.6	1.43	20.1	3.0	0.20	366.2 ± 27
HT > 500 GeV	37.5	1.44	3.6	2.7	0.19	61.6 ± 10.1

The very specific correlation between MHT and the leptons of the decaying W and Z bosons could also be used to extend this strategy to W's and Z's decaying to electrons to increase statistics and cross check results. An alternative strategy would be to use γ + jet events to estimate the Z to invisible background. This is exercised in Ref. [9] for multiple jet searches in SUSY and could also be adopted to this analysis.

5 Conclusions

A prospective search has been carried out for a low mass SUSY signature with dijet events. This analysis represents an extension to the existing SUSY searches at CMS which so far have been based on final states with at least three jets and missing E_{T}. In this study two new kinematic variables, α and α_{T} were explored. These variables are very powerful in suppressing the several orders of magnitude larger background from QCD dijet events without making explicit use of a calorimeter-based missing E_{T} measurement. With the discrimination power of α (α_{T}), several SUSY benchmark points can be discovered with a data sample smaller than 1 fb^{-1}, for which signal-over-background ratios of up to 6 were achieved. Furthermore two independent data-driven techniques have been developped for background estimation. By defining signal-depleted and -enriched regions in the leading jet η it was shown that a matrix method can be used to predict the total number of background events in the central η region with $\alpha_{\mathrm{T}} > 0.55$. In an alternative approach that can be used as a cross-check it was demonstrated how to use W + jets event to determine the dominant $\mathrm{Z} \to \nu\bar{\nu}$ background. Finally, these results show that for a favourable signal like the LM1 benchmark point a discovery would be possible with the early collision data from the LHC.

References

[1] L. Randall and D. Tucker-Smith, "Dijet Searches for Supersymmetry at the LHC," arXiv:0806.1049.

[2] **CMS** Collaboration, G. L. Bayatian et al., "CMS technical design report, volume II: Physics performance," *J. Phys.* **G34** (2007) 995–1579. doi:10.1088/0954-3899/34/6/S01.

[3] https://twiki.cern.ch/twiki/bin/view/CMS/CSA07Physics.

[4] T. Sjostrand et al., "High-energy-physics event generation with PYTHIA 6.1," *Comput. Phys. Commun.* **135** (2001) 238–259, arXiv:hep-ph/0010017. doi:10.1016/S0010-4655(00)00236-8.

[5] M. L. Mangano, M. Moretti, F. Piccinini, R. Pittau, and A. D. Polosa, "ALPGEN, a generator for hard multiparton processes in hadronic collisions," *JHEP* **07** (2003) 001, arXiv:hep-ph/0206293.

[6] W. Beenakker, R. Hopker, M. Spira, and P. M. Zerwas, "Squark and gluino production at hadron colliders," *Nucl. Phys.* **B492** (1997) 51–103, arXiv:hep-ph/9610490. doi:10.1016/S0550-3213(97)00084-9.

[7] https://twiki.cern.ch/twiki/bin/view/CMS/SusyPatCrossCleaner.

[8] **D0** Collaboration, V. M. Abazov et al., "Measurement of dijet azimuthal decorrelations at central rapidities in $p\bar{p}$ collisions at $\sqrt{s} = 1.96$ TeV," *Phys. Rev. Lett.* **94** (2005) 221801, arXiv:hep-ex/0409040. doi:10.1103/PhysRevLett.94.221801.

[9] CMS Physics Analysis Summary, CMS PAS SUS-08-002.

[10] CMS Physics Analysis Summary, CMS PAS EWK-07-002.